



Published in final edited form as:

Laryngoscope. 2011 March ; 121(3): 630–635. doi:10.1002/lary.21414.

TEMPORAL BONE ABNORMALITIES IN CHILDREN WITH *GJB2* MUTATIONS

Margaret A. Kenna, MD, MPH^{1,2}, Heidi L. Rehm, PhD^{1,3,4}, Anna Frangulov, BS¹, Henry A. Feldman, PhD⁵, and Caroline D. Robson, MBChB^{6,8}

¹Dept. of Otolaryngology and Communication Enhancement, Children's Hospital Boston

²Dept. of Otology and Laryngology, Harvard Medical School

³Dept. of Pathology, Brigham and Women's Hospital, Harvard Medical School

⁴Partners Healthcare Center for Personalized Genetic Medicine. Cambridge, MA

⁵Clinical Research Program, Children's Hospital Boston

⁶Dept. of Radiology, Children's Hospital Boston, Harvard Medical School

⁸Department of Pediatrics, Harvard Medical School

Abstract

Objectives—To determine the incidence of temporal bone abnormalities in children with sensorineural hearing loss (SNHL) and pathogenic biallelic *GJB2* mutations.

Study Design—Retrospective analysis of a large cohort of pediatric patients with biallelic *GJB2* mutations and SNHL (observational case series)

Methods—Blinded review of all available temporal bone computed tomographic (CT) and magnetic resonance imaging (MRI) studies in this cohort.

Results—Out of 158 patients with biallelic *GJB2* mutations, **113** had CT and/or MRI studies available for review. Definite, although generally subtle, inner ear abnormalities were present in 12/113. There were malformations of the semicircular canals (SCC) in 4/12, of the internal auditory canal in 2/12, of the cochlear nerve canal (CNC) in 6, and unilateral cochlear malformation in 1/12. MRI in 1/5 showed mildly hypoplastic cochlear nerve. There was no correlation between SNHL severity and presence/absence/type of malformations or genotype.

Conclusions—Our study of 113 biallelic *GJB2* patients with SNHL and temporal bone imaging is the largest study to date. We found only 10% had any abnormalities, most subtle, and none had EVA. Additionally, there was no correlation between SNHL severity and presence/absence/type of malformations or genotype. Disparities between our group and previous reports may be due to differences in degree of hearing loss, types of mutations, populations studied and radiologic factors for both image acquisition and interpretation.

Level of Evidence—2b, Individual retrospective cohort study.

Address correspondence to: Margaret A. Kenna MD, MPH, Dept. of Otolaryngology and Communication Enhancement, Children's Hospital Boston, 300 Longwood Ave. LO-367, Boston, MA 02115, Phone: 617-355-8852, Fax: 617-730-0726, margaret.kenna@childrens.harvard.edu.

Conflict of Interest: none

Keywords

Computed tomography; temporal bones; magnetic resonance imaging; sensorineural hearing loss; *GJB2*; Connexin 26

INTRODUCTION

Sensorineural hearing loss (SNHL), the most common congenital sensory impairment, occurs in 3 out of every 1000 live births¹. Mutations in the gap junction beta 2 (*GJB2*) gene, encoding the connexin 26 (Cx26) protein, are responsible for approximately 20% of all cases of childhood SNHL, with population-specific ranges from 5–85%². The *GJB2* gene, at the DFNB1 locus, was the first identified nuclear gene implicated in nonsyndromic recessive SNHL³. Over 100 mutations have been described to date, with most being recessive and non-syndromic. A small subset are dominant mutations, some of which cause a syndromic presentation involving skin disease (palmoplantar keratoderma).⁴ The initial reports of patients with recessive *GJB2* mutations described bilateral profound SNHL and no other obvious clinical abnormalities.^{3,5} However, marked variability of the audiologic phenotype has now consistently been described in these patients, including age of onset (congenital vs. later onset), asymmetry of the hearing loss (HL), and variability of the degree and configuration of the hearing loss even among siblings with the same mutations. Additionally, progressive and occasionally mixed hearing loss have been described.⁶

Similarly, initial reports described patients with recessive *GJB2* mutations as nonsyndromic and having normal temporal bone computed tomography (CT)^{5,6}. However, as larger numbers of patients with SNHL were evaluated for mutations in *GJB2*, other clinical abnormalities in patients with *GJB2* mutations were reported, although whether these findings are due to *GJB2* mutations, or just coincidental in patients referred to tertiary care pediatric institutions remains unclear^{7,8}. In addition, some reports included occasional descriptions of subtle bony abnormalities on temporal bone CT in patients with *GJB2* mutations⁸. Then, in 2006, Propst et al reported that in their cochlear implant population 53% of ears (72% of subjects) of 53 individuals with biallelic disease-causing *GJB2* mutations had one or more measurable abnormalities of the inner ear as evaluated by CT, including 8% with enlarged vestibular aqueducts (EVA)⁹. This was the first report to describe large numbers of abnormalities seen on temporal bone CT in a *GJB2* population and significantly higher than suggested by others. Subsequently, in 2009, Lee et al. reported on the audiologic and temporal bone findings in their patients with biallelic *GJB2* mutations¹⁰. Although they do not state the number of biallelic *GJB2* patients who had CT of the temporal bones, they report a 5.7% rate of EVA in these patients. In light of these two papers, we report our findings in 113 children with biallelic *GJB2* mutations who underwent imaging of the temporal bones as part of a diagnostic hearing loss evaluation. This represents the largest single institution study of temporal bones findings in children with biallelic *GJB2* mutations and hearing loss.

MATERIALS AND METHODS

Infants and children with sensorineural or mixed hearing loss of any degree who presented to the Dept. of Otolaryngology and Communication Enhancement at the Children's Hospital Boston between December 1998 and December 2008 were eligible for inclusion. As part of the hearing loss evaluation, patients of both genders and all races and ethnicities were offered both imaging of the temporal bones and *GJB2* testing. Initially only children who had a bilateral audiometrically profound clinically nonsyndromic phenotype were offered *GJB2* testing, based on the published literature available at the time. Subsequently, *GJB2*

testing was expanded to include patients with a less severe audiologic phenotype, to those with hearing loss and other clinical findings, and those who had other potential (but unconfirmed) causes of hearing loss. The study was approved by the CHB Institutional Review Board.

Genetic Testing

GJB2 (Connexin 26) testing was performed in the CLIA-approved genetic diagnostic laboratory at CHB. For all tests, genomic DNA was extracted from each patient's blood according to the Genra PureGene (Qiagen, Valencia, CA) protocol. DNA was amplified by polymerase chain reaction (PCR) with two primer sets that amplified the entire open-reading frame of the *GJB2* gene in two overlapping fragments^{7,8}. Each PCR product was then sequenced in both directions using an ABI PRISM® 377 DNA Sequencer (Applied Biosystems, Foster City, CA). Initially, only testing for exon 2 of *GJB2* was offered, but testing for the splice site mutation in exon 1 of *GJB2* was added in April 2006.

After April 2002, all patients were also tested for the *GJB6-D13S1830* (Connexin 30) deletion. (method described in Wu et al, 2003)⁷

Computed Tomography and Magnetic Resonance Imaging

During the study period, CT of the temporal bones was the standard imaging study recommended. However, MRI was often obtained if the CT anatomy was of concern, if the child had neurological abnormalities, if the hearing loss was worsening and other etiologies were suspected, if the child had “no response” to all audiometric testing (suggesting the absence of auditory neural structures) or if the family chose MRI over CT because of concerns about radiation exposure. All available CT and MRI studies were then reviewed, without knowledge of the previous official reading, by a single board certified pediatric neuroradiologist at CHB. Imaging studies were available for review for 113 patients and included CT only in 89 patients, both CT and MR in 19 patients, and MR only in 5 patients. Of the total of 113 CT exams all but 2 were acquired at CHB using either a HiSpeed CTi (General Electric Medical Systems, Milwaukee, WI) or Lightspeed Pro 16 slice multidetector CT (General Electric Medical Systems, Milwaukee, WI). Single detector CT exams consisted of 1 mm thick sequential axial and direct coronal images. Multidetector CT exams consisted of 0.625 mm thick helical axial images reconstructed to 0.75 mm thickness and reformatted coronal images at 1 mm increments. All MR exams were obtained at CHB using a 1.5 Tesla system (General Electric Medical Systems, Milwaukee, WI). Pulse sequences included images of the brain and high resolution 3D axial FSE T2 or 3 D FIESTA images of the temporal bones in the axial and oblique sagittal planes.

CT images were reviewed in detail for anatomy of the inner ear structures including presence of normal cochlear septation, modiolar morphology and transverse axial diameter of the cochlear nerve canal (CNC) as measured on axial images parallel to the plane of the horizontal semicircular canal. A CNC transverse diameter of less than 1.6 mm was considered hypoplastic, based on the average between reports in the literature citing less than 1.4 mm and less than 1.7 mm as abnormal^{11,12}. The size of the vestibular aqueducts was also assessed. Vestibular aqueducts (VAs) were considered enlarged based on a diameter of greater than 1 mm at the midpoint of the VA on the axial images and greater than 2 mm at the opercular level with the measurement technique as previously published¹³. The MR images were similarly assessed for inner ear morphology, fluid signal within the membranous labyrinth, and presence of a normal CN on each size. CN hypoplasia is diagnosed if the CN is smaller in size than the normal ipsilateral facial nerve²¹⁴.

RESULTS

158 patients with biallelic *GJB2* mutations were identified. 113/158 had temporal bone CT and/or MRI obtained between 1998 and 2008 and available for review. Images were not available for the remaining 45 because the family had chosen not to proceed with CT/MRI or the films performed were not available. Reasons parents cited for not wanting imaging included concerns about sedation or radiation exposure, insurance coverage, and questions about the utility of the study.

Of the 113 CT scans evaluated, 12 had inner ear abnormalities. (TABLE 1). 4/12 patients had abnormalities of the semicircular canals (SCC), including globular enlargement of the horizontal SCC (1), thickened horizontal SCC (2) and dysmorphic SCC with small horizontal SCC (1). Two patients had asymmetry of the internal auditory meati. The left measured 3.6 mm in anteroposterior (AP) diameter at its midpoint on the left and 5.7 mm on the right on axial images, with a narrowest superoinferior (SI) diameter of 1.1 mm at the porus acousticus on the coronal images on the left. This patient also had bilateral mild CNC hypoplasia. The second had mild asymmetry with midpoint AP diameters of approximately 2.6 mm on the right and 3.2 mm on the left with narrowest SI measurements of 2 mm bilaterally at the level of the porus acousticus. One patient had unilateral deficiency of the modiolus without EVA with ipsilateral CNC hypoplasia with a diameter of 1.6 mm. Five patients had mild bilateral CNC hypoplasia with diameters of 1.4 – 1.5 mm. MR was obtained in one of the patients with CNC hypoplasia and revealed mild bilateral cochlear nerve hypoplasia. One additional patient had a cerebellar astrocytoma (seen on MRI) felt to be unrelated to their *GJB2* status. All 12 patients had bilateral congenital sensorineural hearing loss, four severe to profound, three moderate to severe, two mild to moderate, one moderate, one mild to severe and one mild. Four of the twelve have had cochlear implants and all are successful users.

There was no statistical difference in the four frequency pure tone audiometric average (500Hz, 1000Hz, 2000Hz, 4000Hz, PTA) for patients with or without temporal bone abnormalities. (Table 2) Significantly worse hearing by PTA was noted for the truncating (T) vs. the non-truncating (NT) mutations: T/T (94dB±22), T/NT (57dB±35) and NT/NT (34dB±21) $p<0.0001$ by Kruskal-Wallis test for three way comparison. However, there was no difference between the presence or absence of temporal bone abnormalities related to the presence of truncating or non-truncating mutations, $p=0.51$ by Fisher Exact test for a comparison of the T/T, T/NT, and NT/NT groups.

Fifty-four patients had both CT and a sufficient number of audiograms to assess for progression of the hearing loss. Of the 8/54 who had an abnormal CT, 5 (63%) had a progressive hearing loss. Among the 46/54 who had a normal CT, 25 (54%) had a progressive hearing loss. The difference is non-significant by Fisher Exact Test, $p=.72$.

DISCUSSION

Patients with SNHL and biallelic *GJB2* mutations may have temporal bone abnormalities detectable by CT or MRI. In our study, we found a much smaller number of patients with temporal bone abnormalities, comprising approximately 10% of our patients with *GJB2* mutations, than did Propst et al, 2006⁹. In contrast to both Propst et al and Lee et al, we did not find any patients with EVA^{9,10}. Our patients, similar to the Lee et al study, had a wide spectrum of degree of hearing loss; 61% were bilateral severe to profound, and 39% were in the mild to moderately-severe range at the time of presentation¹⁰. In contrast, Propst et al studied only their cochlear implant population, so presumably they all had bilateral profound SNHL⁹. This raises the question whether patients with a more severe degree of hearing loss

are more likely to have temporal bone abnormalities. Other possibilities for the variation between our results and others include differences in CT/MRI techniques and in the guidelines used for evaluating the films. Population differences may also be a factor.

Mutations in *GJB2* are the most common genetic cause of congenital and childhood onset SNHL. Original reports of *GJB2* deafness described normal temporal bone CT, no other associated clinical findings, and bilateral profound congenital hearing loss^{5,6}. Since the initial *GJB2* studies were published in 1997, multiple authors and research groups have described many populations with *GJB2* mutations. The papers support over 100 recessive mutations and at least 9 dominant mutations, several of which are syndromic. The patients have a highly variable audiologic phenotype, including variable age of onset, asymmetry of the hearing loss, and progression of the hearing loss. However, with the exception of the Propst et al study, no other study describes large numbers of *GJB2* patients with imaging abnormalities⁹. Our study describes abnormalities of the temporal bones in 10% of patients with biallelic *GJB2* mutations; most of the findings were subtle, and none had EVA. Similar to recent studies describing the presence of other clinical findings in patients with *GJB2* deafness, it is unclear whether the CT findings are due to the *GJB2* mutations, or whether they are a coincidental finding⁸.

Anatomic abnormalities of the temporal bones, as detected by both CT and magnetic resonance imaging (MRI), have been reported with increasing frequency in patients with hearing loss. This is due to improved imaging techniques, increased awareness of the association between these structural abnormalities and hearing loss, the need to identify abnormalities in patients who may be cochlear implant candidates, and the need for diagnostic information upon which to base prognosis and counseling. Temporal bone abnormalities are found in both syndromic and non-syndromic patients. For example, Pendred syndrome, initially described as congenital profound hearing loss, goiter, and thyroid dysfunction, has been found to be due to recessive mutations in the *SLC26A4* gene. Patients with both syndromic and non-syndromic (DFNB4) biallelic *SLC26A4* mutations nearly always have temporal bone abnormalities, most commonly enlarged vestibular aqueducts and incomplete cochlear partition (“Mondini dysplasia”)¹⁵. Hearing loss in these patients ranges from mild to profound and can be very asymmetric. Other hearing loss syndromes with well-described temporal bone abnormalities include branchio-oto-renal syndrome due to mutations in the *EYA1* and *SIX5* genes, CHARGE syndrome, usually associated with mutations in the *CHD7* gene, and Waardenburg syndrome, caused by mutations in several genes including *PAX3*, *MITF*, *SNA12*, *EDNRB*, *EDN3* and *SOX10*¹⁶.

The degree and configuration of hearing loss found in association with anatomic inner ear abnormalities varies from mild to profound. The patient population in the current report with biallelic *GJB2* mutations also had hearing loss ranging from bilateral mild to profound. However, there was no relationship between the degree of hearing loss and the presence or absence of temporal bone abnormalities in the biallelic *GJB2* patients; in addition, there was no statistical relationship between progression of hearing loss and the presence or absence of temporal bone abnormalities in the biallelic *GJB2* patients.

The recent report by Propst et al, on cochlear implant recipients with biallelic *GJB2* mutations found that 72% of subjects (53% of ears) had at least one measurable temporal bone abnormality⁹. The most common findings were 1. dilated endolymphatic fossa (28%); 2. hypoplastic modiolus (25%); 3. large vestibular aqueduct (8%); 4. hypoplastic horizontal semicircular canal (8%); and 5. hypoplastic cochlea (4%). All of these patients had bilateral profound SNHL, so a relatively high incidence of anatomic abnormalities may not be surprising. However, these authors report that a subset of 21 patients from the *GJB2* group were age matched and compared with 21 one controls without hearing loss, and that

temporal bone abnormalities were detected in 55 % of the *GJB2* group and 29% of controls. This study reports an unusually high percentage of abnormalities in their control population. However, the authors reported that the incidence of anatomic abnormalities in patients with *GJB2* mutations was higher than in those without mutations, suggesting a possible relationship between the two. A question then arises as to what should be considered abnormal on imaging exams. In a recent report by Vijayasekaran et al, the VA midpoint and opercular widths were measured on CT in 73 children with normal hearing¹³. These authors concluded that midpoint and opercular widths of 1.0 mm and 2.0 mm or greater respectively should be considered enlarged. In measuring the opercular width, particular attention should be given to the technique utilized by Vijayasekaran et al which is reproducible and avoids the pitfall of considering mildly flared VA opercular segments as abnormal. The significance of borderline enlargement of the opercular width, in the presence of a normal midpoint width is uncertain, particularly in infants in whom further ossification around the operculum can occur as part of normal temporal bone development. In our institution patients in whom only the opercular diameter of the VA is borderline enlarged are referred for MR imaging. If MRI fails to show enlargement of the endolymphatic sac and duct then the flared opercular margin of the VA is not considered significant.

In addition to VA opercular changes that occur with age, there is also some variability in appearance of the temporal bone with age with respect to the presence of pericochlear lucency, and apparent deficiency of the bone over the semicircular canals. Sequential imaging that was obtained in a small number of patients in this series revealed maturational changes that included resolution of pericochlear lucency, normalization of the width of the operculum of the VA and thickening of the bone over the superior and posterior semicircular canals. The presence of lucency around the cochlea is considered a normal finding. Chadwell et al described a cleft that appears as a lucency parallel to the lateral aspect of the cochlea on CT in young patients¹⁷. They attributed this finding to a space between the endosteal and outer periosteal layers of the otic capsule or possibly related to the fissula ante fenestram. A CT diagnosis of dehiscence of the semicircular canals has been reported to have a positive predictive value of 57 % and the prevalence of dehiscent appearing semicircular canals on high resolution, thin section CT is much higher than anticipated by pathologic studies, suggesting that there is a tendency to over diagnose this entity on CT¹⁸.

Russo et al reported on MRI temporal bone findings in children with bilateral profound SNHL as well as children with normal hearing¹⁹. They found that children with profound SNHL of unknown cause, as well as children with *GJB2* mutations, had a higher incidence of hypoplastic cochlear nerves compared to normal hearing controls. One of the seven children with *GJB2* mutations was compound heterozygous and the others heterozygous. One of the patients with a single *GJB2* mutation also had skin disease, making it likely that this patient had a dominant syndromic form of *GJB2* deafness.

A mechanism that might result in temporal bone abnormalities in patients with *GJB2* mutations is unclear. Abnormalities of the membranous cochlear and vestibular structures are generally found in association with bony abnormalities, but may also be present when the bony structures appear normal (at least by CT). There are few microscopic studies of temporal bone anatomy in patients with SNHL and *GJB2* mutations. Griffith et al reported on the temporal bones in a male infant with keratitis-ichthyosis-deafness (KID) syndrome, an autosomal dominant syndrome due to *GJB2* mutations²⁰. In this subject, who was heterozygous for G45E, a previously reported dominant KID syndrome mutation in *GJB2*, they found dysplasia of the cochlear and saccular neuroepithelium³²⁰. Jun et al looked at one human temporal bone in the Univ. of Iowa temporal bone collection. The patient was compound heterozygous for two *GJB2* mutations, (35delG/E101G). They found no neural degeneration, a good population of spiral ganglion cells, near-total degeneration of hair cells

in the organ of Corti, a detached and rolled-up tectorial membrane, agenesis of the stria vascularis, and a large cyst in the scala media in the region of the stria vascularis²¹. Kudo et al generated a transgenic mouse model that expressed a mutant *GJB2* with a R75W mutation (a dominant cause of *GJB2* SNHL)²². These mice had severe to profound hearing loss, deformity of supporting cells, failure in the formation of the tunnel of Corti and degeneration of sensory hair cells. However, no obvious structural change was observed in the stria vascularis or spiral ligament, despite strong expression of *GJB2* in those areas. The high resting potential in cochlear endolymph necessary for hair cell function was maintained. The authors suggested that this *GJB2* mutation disrupted cortilymph homeostasis due to impaired potassium transport by supporting cells, resulting in degradation of the organ of Corti, rather than affecting endolymph homeostasis. It is possible to see that different mutations in *GJB2*, depending on expression and function in the cochlea, may result in differing degrees of hearing loss, as well as varying structural and functional abnormalities.

Imaging of the temporal bone is an integral part of the hearing loss evaluation. There are many reasons children with *GJB2* mutations may need to undergo temporal bone imaging, including consideration for cochlear implant, history of head trauma or meningitis, or for other medical or surgical reasons. Further, both Russo et al¹⁹ as well as Adunka et al²³ have reported that temporal bone CT alone may underestimate, or miss entirely, abnormalities of the cochlear nerve. Interestingly, in our patients, mild hypoplasia of the CN canal was the most frequent abnormality and occurred bilaterally in 6 and unilaterally in 1 patient. MR was only available in 1 of these patients and confirmed mild cochlear nerve hypoplasia. However the clinical significance of the finding is uncertain. In addition there is no consensus as to an absolute transverse CNC diameter that should be considered abnormal with measurements ranging from less than 1.4 mm to less than 1.8 mm^{9,11,12}. However the criteria for diagnosing cochlear nerve hypoplasia on MRI seems more straightforward. Evaluating the cochlear nerves is especially important in children who are being evaluated for cochlear implantation. Both genetic evaluation and temporal bone imaging are therefore important in the diagnostic assessment of the child with SNHL.

CONCLUSIONS

Approximately 10% (12/113) of our patients with biallelic *GJB2* mutations had abnormalities of the temporal bone detected on CT or MRI. Most findings were subtle and no patients had EVA. In addition, there was no statistical relationship between the presence or absence of temporal bone abnormalities and either the degree or progression of the hearing loss. Given the high prevalence of both *GJB2* mutations and imaging abnormalities in the hearing loss population, it is statistically likely that both will occasionally be found in the same patients. Therefore, our results do not yet support *GJB2* mutations as a clear cause of anatomic abnormalities of the temporal bones. Rapid advances in hearing loss genetics and imaging make the relationship between the two an important area of further study.

Acknowledgments

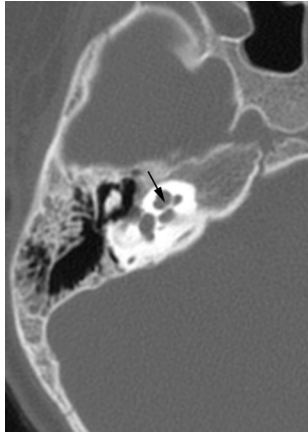
Supported by a grant from the National Institute for Deafness and Other Communication Disorders. NIDCD R01 DC05248 (Dr. Kenna)

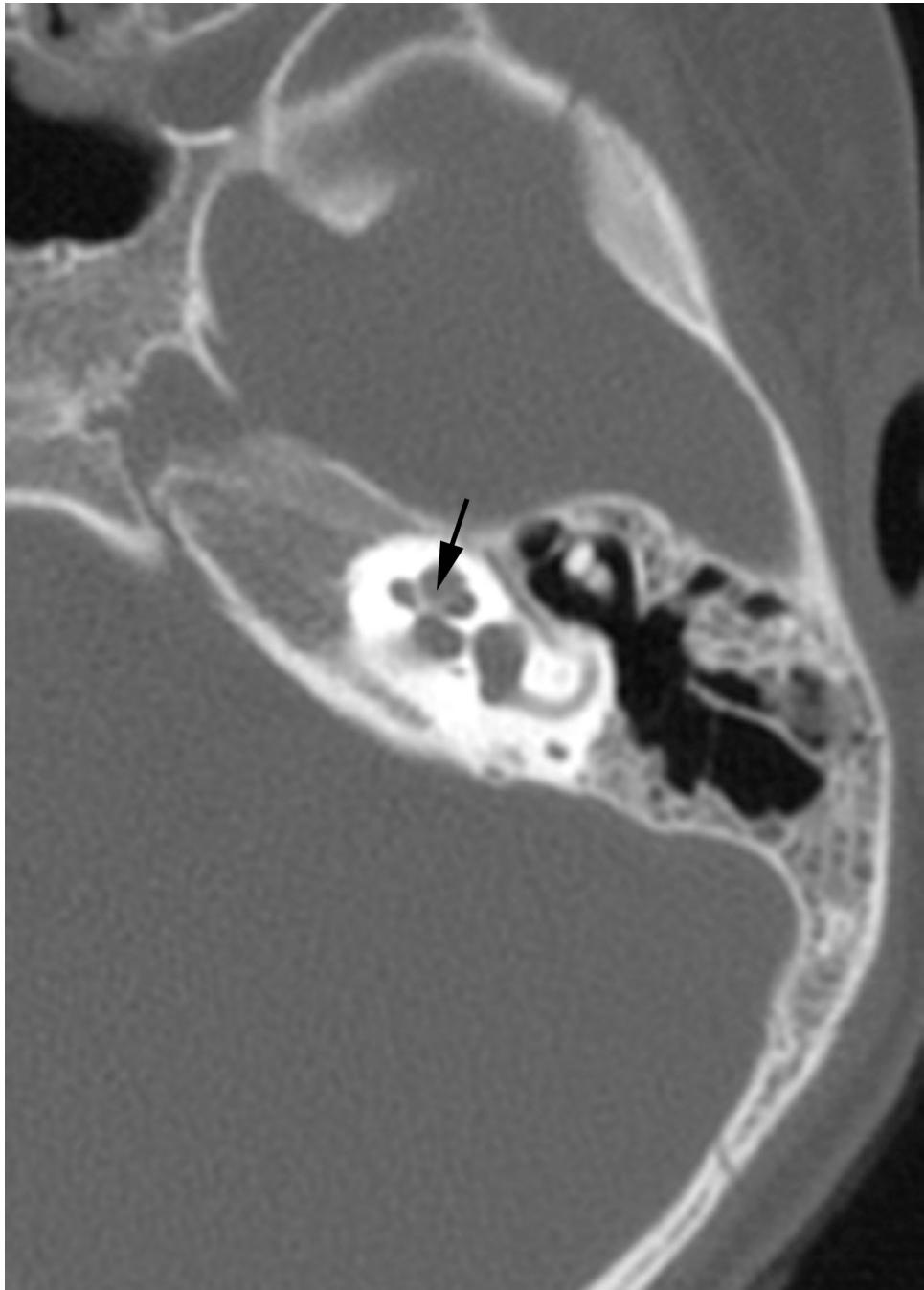
REFERENCES

1. NCHAM. National Center for Hearing Assessment and Management. [Accessed August 29, 2010]. <http://www.infanthearing.org>.
2. Kenneson A, Van Naarden Braun K, Boyle C. GJB2 (connexin 26) variants and nonsyndromic sensorineural hearing loss: a HuGE review. *Genet Med*. 2002; 4(4):258–274. [PubMed: 12172392]

3. Kelsell DP, Dunlop J, Stevens HP, et al. Connexin 26 mutations in hereditary non-syndromic sensorineural deafness. *Nature*. 1997; 387(6628):80–83. [PubMed: 9139825]
4. Ballana, E.; Ventayol, M.; Rabionet, R.; Gasparini, P.; Estivill, X. Connexins and Deafness Homepage. [Accessed Oct. 20, 2010]. <http://davinci.crg.es/deafness>.
5. Green GE, Scott DA, McDonald JM, Woodworth GG, Sheffield VC, Smith RJ. Carrier rates in the midwestern United States for GJB2 mutations causing inherited deafness. *JAMA*. 1999; 281(23): 2211–2216. [PubMed: 10376574]
6. Cohn ES, Kelley PM, Fowler TW, et al. Clinical studies of families with hearing loss attributable to mutations in the connexin 26 gene (GJB2/DFNB1). *Pediatrics*. 1999; 103(3):546–550. [PubMed: 10049954]
7. Kenna MA, Feldman H, Neault MW, Frangulov A, Wu B-L, Fligor B, Rehm HL. Audiologic Phenotype and Hearing Loss Progression in Children with Connexin 26 Mutations. *Arch Otolaryngol Head Neck Surg*. 2010 Jan; 136(1):81–87. [PubMed: 20083784]
8. Kenna MA, Rehm HL, Frangulov A, Yaeger D, Krantz ID. Additional clinical manifestations in children with sensorineural hearing loss and biallelic GJB2 mutations: who should be offered connexin 26 testing? *Am J Med Genet A*. 2007; 143A(14):1560–1566. [PubMed: 17455295]
9. Propst EJ, Blaser S, Stockley TL, Harrison RV, Gordon KA, Papsin BC. Temporal bone imaging in GJB2 deafness. *Laryngoscope*. 2006; 16(12):2178–2186. [PubMed: 17146393]
10. Lee KH, Larson DA, Shott G, et al. Audiologic and temporal bone imaging findings in patients with sensorineural hearing loss and GJB2 mutations. *Laryngoscope*. 2009; 119(3):554–558. [PubMed: 19235794]
11. Fatterpekar GM, Mukherji SK, Lin Y, Alley JG, Stone JA, Castillo M. Normal canals at the fundus of the internal auditory canal: CT evaluation. *J Comput Assist Tomogr*. 1999; 23(5):776–780. [PubMed: 10524866]
12. Stjernholm C, Muren C. Dimensions of the cochlear nerve canal: a radioanatomic investigation. *Acta Otolaryngol*. 2002; 122(1):43–48. [PubMed: 11876597]
13. Vijayasekaran S, Halsted MJ, Boston M, et al. When is the vestibular aqueduct enlarged? A statistical analysis of the normative distribution of vestibular aqueduct size. *Am J Neuroradiol*. 2007; 28(6):1133–1138. [PubMed: 17569973]
14. McClay JE, Booth TN, et al. Evaluation of pediatric sensorineural hearing loss with magnetic resonance imaging. *Arch Otolaryngol Head Neck Surg*. 2008; 134(9):945–952. [PubMed: 18794439]
15. Usami S, Abe S, Weston MD, Shinkawa H, Van Camp G, Kimberling WJ. Non-syndromic hearing loss associated with enlarged vestibular aqueduct is caused by PDS mutations. *Hum Genet*. 1999; 104(2):188–192. [PubMed: 10190331]
16. Van Camp, G.; Smith, R. Hereditary Hearing Loss Homepage. [Accessed Oct. 20, 2010]. Available from: <http://hereditaryhearingloss.org>.
17. Chadwell JB, Halsted MJ, Choo DI, Greinwald JH, Benton C. The cochlear cleft. *AJNR Am J Neuroradiol*. 2004; 25(1):21–24. [PubMed: 14729522]
18. Cloutier JF, Bélair M, Saliba I. Superior semicircular canal dehiscence: positive predictive value of high-resolution CT scanning. *Eur Arch Otorhinolaryngol*. 2008; 265(12):1455–1460. [PubMed: 18415114]
19. Russo EE, Manolidis S, Morriss MC. Cochlear nerve size evaluation in children with sensorineural hearing loss by high-resolution magnetic resonance imaging. *Am J Otolaryngol*. 2006; 27(3):166–172. [PubMed: 16647980]
20. Griffith AJ, Yang Y, Pryor SP. Cochleosaccular dysplasia associated with a connexin 26 mutation in keratitis-ichthyosis-deafness syndrome. *Laryngoscope*. 2006; 116(8):1404–1408. [PubMed: 16885744]
21. Jun AI, McGuirt WT, Hinojosa R, Green GE, Fischel-Ghodsian N, Smith RJ. Temporal bone histopathology in connexin 26-related hearing loss. *Laryngoscope*. 2000; 110(2 Pt 1):269–275. [PubMed: 10680928]
22. Kudo T, Kure S, Ikeda K, et al. Transgenic expression of a dominant-negative connexin26 causes degeneration of the organ of Corti and non-syndromic deafness. *Hum Mol Genet*. 2003; 12(9): 995–1004. [PubMed: 12700168]

23. Adunka OF, Roush PA, Teagle HF, et al. Internal auditory canal morphology in children with cochlear nerve deficiency. *Otol Neurotol*. 2006; 27(6):793–801. [PubMed: 16936566]







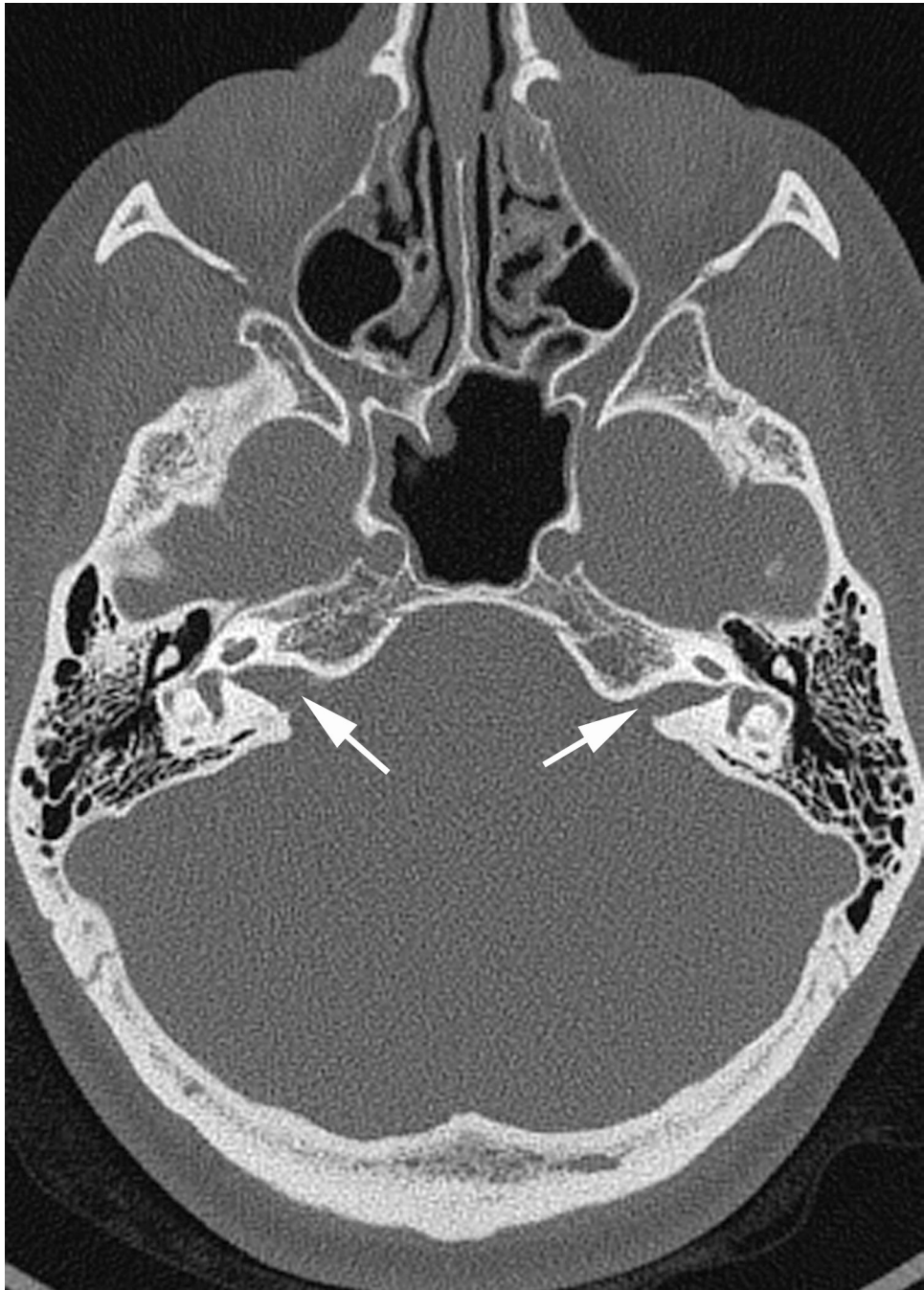


**Fig. 1.**

(a) Axial temporal bone CT at the level of the cochlea reveals deficiency of the posterolateral struct of the right modiolus (arrow). (b) The normal left modiolus (arrow) in the same patient (Fig. 1a) is shown for comparison. (c) Axial temporal bone CT at the level of the vestibule demonstrates mild enlargement of the left vestibule with a malformed, mildly thickened horizontal semicircular canal (arrow) that contains a smaller than usual bone island; (d). Axial temporal bone CT shows asymmetry in the shape and size of the internal auditory meati (arrows) with the left appearing narrower than the right. (e) reformatted coronal CT in the same patient (Fig. 1d) demonstrates moderate narrowing of the medial aspect of the right internal auditory meatus (arrow).

Table 1

Patients with biallelic GJB2 mutations and abnormal CT or MR imaging

Gender	Age	Findings	GJB2 Mutations
M	13y	Rt IAC 2.6 mm width < Lt 3.2; CNC: Rt 1.5 mm, Lt 1.5 mm	V37I/V37I
M	15y	Thickened Lt HSCC	V37I/V37I
F	6m	Globular horiz SCC Lt > Rt	35delG/35delG
M	2y	Mildly thickened HSCC	35delG/Q57X
F	11y	Slightly small vestibule and dysmorphic scc small horizontal scc	35delG/35delG
F	19y	Lt IAC 3.6 mm width < Rt 5.7 mm, Lt: 1mm on coronals	35delG/35delG
F	3y	Deficiency posterolateral struct Rt modiolus; CNC Rt 1.4 mm Lt 1.6 mm	35delG/M34T
M	2y	CNC: Rt 1.5 mm, Lt 1.4 mm, cochlear nerves mildly hypoplastic on MR	35delG/167delT
F	5m	CNC: Rt 1.5 mm, Lt 1.5 mm	35delG/M34T
F	4m	CNC: Rt 1.5 mm, Lt 1.5 mm	L90P/453-460del8ins9
F	6y	CNC: Rt 1.5 mm, Lt 1.5 mm	V37I/V37I
F	4m	CNC: Rt 1.5 mm, Lt 1.5 mm	35delG/35delG

LT=left; RT=right

Table 2

PTA Data for Subjects with Abnormal and Normal CT Studies.

CT	N OBS	Mean PTA	Standard Deviation	Median PTA	Lower Quartile	Upper Quartile	Minimum	Maximum
Abnormal*	12	61.25	29.25	61.25	35.63	81.25	23.75	116.30
Normal*	101	76.75	35.02	95.00	38.75	103.8	11.25	125.00

* There is no statistical difference between these two groups by either the Student T-Test or Wilcoxon Test, both p=0.11.